Published in final edited form as:
Virology. 2011 April 10; 412(2): 392–400. doi:10.1016/j.virol.2011.01.028.

The Epstein-Barr Virus BART microRNAs target the pro-apoptotic protein Bim

Aron R. Marquitz[a], **Anuja Mathur**[a], **Cyd Stacy Nam**[a], and **Nancy Raab-Traub**[a,b,§]

Aron R. Marquitz: arm6@med.unc.edu; Anuja Mathur: anujam@email.unc.edu; Cyd Stacy Nam: cn_nam@yahoo.com; Nancy Raab-Traub: nrt@med.unc.edu

[a] Lineberger Comprehensive Cancer Center, University of North Carolina at Chapel Hill, Chapel Hill, North Carolina 27599

[b] Department of Microbiology-Immunology, University of North Carolina at Chapel Hill, Chapel Hill, North Carolina 27599

Abstract

In Epstein-Barr virus infected epithelial cancers, the alternatively spliced BamHI A rightward transcripts (BARTs) are abundantly expressed and are the template for two large clusters of miRNAs. This study indicates that both of these clusters independently can inhibit apoptosis in response to etoposide in an epithelial cell line. The Bcl-2 interacting mediator of cell death (Bim) was identified using gene expression microarrays and bioinformatic analysis indicated multiple potential binding sites for several BART miRNAs in the Bim 3'UTR Bim protein was reduced by Cluster I and the individual expression of several miRNAs, while mRNA levels were unaffected. In reporter assays, the Bim 3' untranslated region (UTR) was inhibited by both clusters but not by any individual miRNAs. These results are consistent with the BART miRNAs downregulating Bim post-transcriptionally in part through the 3'UTR and suggest that there are miRNA recognition sites within other areas of the Bim mRNA.

Keywords

EBV; miRNA; apoptosis; Bim; BART

INTRODUCTION

Epstein-Barr Virus (EBV) is a member of the Herpes virus family that infects greater than 90% of the human population yet is associated with a number of malignancies (Rickinson and Kieff, 2001). These cancers develop in both epithelial and lymphoid cells and include Burkitt's lymphoma (BL), Hodgkin's disease, post-transplant lymphoma, nasopharyngeal carcinoma (NPC), and gastric carcinoma (Fukayama, Hino, and Uozaki, 2008; Raab-Traub, 2002; Young and Murray, 2003). EBV expression within the tumors is predominantly latent with expression of a small subset of the more than 100 genes potentially encoded by the virus. There are at least three distinct forms of latent infection marked by different patterns of viral gene expression. The viral genes expressed in the cancers are thought to contribute to the induction of uncontrolled cellular growth and several of these proteins have

[§]Corresponding Author: Phone: (919) 966-1701, Fax: (919) 966-9673.

transforming properties *in vitro*. Recently it has been discovered that EBV also encodes for at least 25 microRNAs (miRNAs), many of which are highly expressed during latency (Cai et al., 2006; Grundhoff, Sullivan, and Ganem, 2006; Pfeffer et al., 2004; Zhu et al., 2009). It is likely that these miRNAs contribute to the growth changes induced during EBV latent infections. Uncovering the function of these miRNAs may identify new mechanisms by which EBV infection leads to transformation and malignancy.

miRNAs are approximately 22 nucleotide long noncoding RNAs that closely resemble small interfering RNAs (siRNAs) in size and function. However, unlike siRNAs, miRNAs are most often generated from RNA polymerase II transcripts in higher eukaryotes, which are processed by the RNase III enzyme Drosha/DGCR8 complex to form approximately 60 nucleotide hairpin precursors known as pre-miRNAs (Bartel, 2004; Cullen, 2006). The pre-miRNAs are exported to the cytoplasm via Exportin 5 where the mature form of the miRNA is cleaved out of the hairpin by the RNase III enzyme Dicer (Bartel, 2004; Cullen, 2006). The mature miRNA is then incorporated into a protein complex known as the RNA-induced silencing complex (RISC) and targeted to the 3'UTR of an mRNA based on base pair complementarity, most importantly with nucleotides 2–8 of the miRNA, which is known as the seed sequence (Bartel, 2004; Cullen, 2006). The binding of the miRNA/RISC complex to the 3'UTR of the target mRNA was originally thought to repress translation of the targeted mRNA with partial complementarity to the target site or promote mRNA degradation with complete complementarity (Bartel, 2004). Multiple studies indicate that expression can be targeted in both ways. Transfection of miRNAs into cells identified decreased levels of many mRNAs containing seed sequence matches to the particular miRNAs (Lim et al., 2005). Additionally, a recent study comparing mRNA sequencing data with proteomic data sets suggested that at least for several human miRNAs, changes in mRNA levels and not changes in rates of translation, correlated to changes in protein levels (Guo et al., 2010). However, in multiple instances in which specific miRNA targets have been examined on an individual basis, regulation primarily occurs at the protein level without a corresponding decrease in mRNA levels. Significantly, this mode of regulation has been demonstrated for several viral miRNAs, such as miR-H2-3p and miR-H6 of HSV-1, which are able to decrease viral expression exclusively at the protein level (Umbach et al., 2008).

The EBV miRNAs are produced as two clusters from RNAs that are also differentially expressed in the different latent expression patterns. Three miRNA precursors are encoded near the BHRF1 gene and are apparently produced from an intron within the long EBNA transcript (Cai et al., 2006). These miRNAs have only been detected in Type 3 latency that is characteristic of transformed B-lymphocytes and post-transplant lymphoma. The remaining 22 precursors are encoded in the introns of the Bam HI A region rightward transcripts (BARTs) (Cai et al., 2006; Grundhoff, Sullivan, and Ganem, 2006; Pfeffer et al., 2004; Zhu et al., 2009). The BART transcripts were originally identified in NPC (Gilligan et al., 1990; Hitt et al., 1989) and are most abundant in Type 1 and Type 2 latency, the more restricted patterns of EBV latent infection that are characteristic of the majority of the EBV associated cancers (Rickinson and Kieff, 2001). Multiple studies have used quantitative RT-PCR to examine the expression of EBV miRNAs in multiple cell lines, disease states, tumor samples and during lytic reactivation (Amoroso et al., ; Cosmopoulos et al., 2009; Pratt et al., 2009). These studies have largely supported the data generated from Northern blots and direct cloning/sequencing methods with regard to the patterns of EBV miRNA expression and have revealed heterogeneity in the relative abundance of individual miRNAs in different cell lines or samples (Cai et al., 2006; Edwards, Marquitz, and Raab-Traub, 2008; Kim do et al., 2007; Lung et al., 2009; Zhu et al., 2009).

Potential functions have been identified for some of the EBV miRNAs. Several of the miRNAs negatively regulate viral transcripts. miR-BART2 is encoded antisense to the 3'UTR of the viral DNA polymerase, BALF5, and thus has perfect complementarity to the BALF5 transcript and can decrease the levels of mRNA and protein (Barth et al., 2008). Both latent membrane protein 1 and 2 (LMP1 and 2) are decreased by BART miRNAs through imperfect complementary sites in the 3'UTRs of their respective transcripts (Lo et al., 2007; Lung et al., 2009). A few cellular targets have also been identified. miR-BHRF1-3 targets the T-cell attracting chemokine, CXCL-11 (Xia et al., 2008). miR-BART2 also targets the stress induced molecule MICB (Nachmani et al., 2009). Additionally, miR-BART5 has been shown to target p53 up-regulated modulator of apoptosis (PUMA), a proapototic protein belonging to the BH3-only class of the Bcl-2 family, and inhibit apoptosis (Choy et al., 2008).

In this study, the BART miRNAs coding region was cloned in two constructs and expressed exogenously in the AGS gastric carcinoma cell line, a cell line that can be infected with EBV resulting in altered growth properties (Kassis et al., 2002). In these cell lines, both BART constructs inhibited apoptosis in response to etoposide treatment, suggesting that multiple miRNAs regulate this process. Using a combination of microarray and bioinformatic analysis, several potential targets of the BART miRNAs were identified that could contribute to the protection from apoptosis. Of these potential targets, multiple miRNA predicted binding sites were identified for the Bcl-2 interacting mediator of cell death (Bim) and Bim protein was decreased in cell lines expressing several of the BART miRNAs.

RESULTS

Generation of epithelial cell lines that express the EBV BART miRNAs

To determine the role of EBV BART miRNAs in promoting epithelial cell cancers, pcDNA3 constructs that express the two clusters of BART miRNAs with different selectable markers were stably expressed in AGS cells, a human gastric carcinoma derived cell line (Barranco et al., 1983). Four cell lines were created including a control with the two pcDNA3 vectors, a cell line that contains both clusters, and two cell lines that express each cluster individually in addition to the appropriate control vector (Figure 1). Expression of the miRNAs was determined using Northern blotting and qRT-PCR in comparison with the C666-1 NPC cell line (Cheung et al., 1999). This cell line expresses high levels of the BART miRNAs and has been used as the reference level in most studies that have quantified the BART miRNAs. Northern blotting identified expression of miR-BART4 from Cluster I and miR-BART9 from Cluster II (Figure 2A). miR-BART4 was expressed at levels slightly lower than in C666-1 cells, however, miR-BART9 was expressed at slightly higher levels than C666-1 cells.

In order to confirm expression observed through Northern blotting and expand this data to additional miRNAs, the Qiagen miScript system for qRT-PCR of miRNAs was used. To validate the ability of this system to accurately measure relative abundance of EBV miRNAs; C666-1 total cellular RNA, which contains abundant EBV miRNAs, was diluted to varying degrees with AGS total cellular RNA, which does not contain EBV miRNAs. PCR was then performed for nine different BART miRNAs using an equal amount of total RNA input but with varying concentrations of C666-1 RNA (and thus varying concentrations of BART miRNAs). Cycle thresholds (C_Ts) obtained were compared to theoretical results based on the fraction of the input RNA that originated from C666-1 cells, where the expected C_T was equal to the C_T obtained from undiluted C666-1 RNA plus $\log_2$ [total RNA]/[C666-1 RNA]. In the majority of cases, the qRT-PCR performed very well, with C_Ts increasing at the expected rate as the amount of C666-1 RNA decreased (Figure

2B). In a few instances the measured C_Ts were larger than the expected at some dilutions; suggesting that with decreasing concentrations of miRNAs, this system for PCR may underestimate the level of expression of some miRNAs. However, it should be possible to use this system to determine the relative level of expression of BART miRNAs compared to C666-1 cells with reasonable confidence. Evaluation of these nine individual miRNAs representative of both clusters in the AGS stable cells confirmed expression of the multiple miRNAs in each cell line and corroborated the Northern blot data, with miRNAs from Cluster I expressed at levels slightly lower than C666-1 cells and miRNAs from Cluster II expressed at the same to slightly higher levels than C666-1 cells (Figure 2C). Importantly, these data indicated that the AGS stable cell lines express the EBV BART miRNAs at physiologically relevant levels.

Both Clusters of BART miRNAs are capable of inhibiting apoptosis

In order to determine potential effects of the BART miRNAs in inhibiting apoptosis, the cell lines expressing the BART miRNAs were treated with etoposide, an inhibitor of topoisomerase II, that is known to induce apoptosis in a wide variety of cells (Montecucco and Biamonti, 2007; van Maanen et al., 1988). Cells expressing both clusters of miRNAs were treated with two concentrations of etoposide for 24 hours, and apoptosis was measured by PARP cleavage (Figure 3A). Cells expressing the miRNAs had more uncleaved PARP at both concentrations. To identify which cluster is responsible for this inhibition, apoptosis was induced in all four AGS cell lines at both concentrations of etoposide (Figure 3B). Strikingly, cells containing either cluster of miRNAs had more uncleaved PARP than control cells at both concentrations. Determination of the percentage of cleaved PARP relative to total PARP indicated that the individual clusters and in combination had considerably less cleaved PARP compared to the total (Figure 3C). Analysis of the same lysates for caspase-3 revealed decreased levels of the cleaved and activated form in cells expressing either miRNA clusters (Figure 3B). These findings indicate that miRNAs in both clusters can protect the AGS cells from apoptotic stimuli.

Microarray analysis of AGS cells expressing miRNAs

To determine how the BART miRNAs inhibit apoptosis it is essential to identify the cellular transcripts that are targeted by specific miRNAs. Some miRNA targets have been successfully identified through the use of expression microarrays (Lim et al., 2005). However, this approach is difficult as many targeted mRNAs either do not decrease in abundance or are only slightly decreased and are likely to not be detected by array. One approach has been to use multiple mRNA microarray analyses to obtain statistical significance and several miRNA targets have been successfully identified in this way (Gottwein et al., 2007; Samols et al., 2007; Ziegelbauer, Sullivan, and Ganem, 2009).

Four replicate whole genome expression microarrays were performed on the cells expressing both clusters of miRNAs. The effects on mRNA levels were small with no potential targets having statistical significance of $p<0.05$ in a standard t-test. Of the genes with detectable expression on the array, 944 genes had gene ontology annotations indicating involvement in apoptosis. Of these, 133 genes were decreased in all four arrays compared to control cells (Supplementary Table 1). Six of these genes; PUMA, Bim, Bik, BNIPL, HRK, and Bcl-G; belonged to the BH3-only group of the Bcl2 family. The BH3-only proteins are pro-apoptotic members of the larger Bcl2 family that control the release of cytochrome c from the mitochondria and thus are central regulators of apoptosis (Lomonosova and Chinnadurai, 2008). The detection of PUMA using this approach was consistent with the previous identification that PUMA was a target of miR-BART5 (Choy et al., 2008).

To address whether any of these BH3-only genes are direct targets of the BART miRNAs, the 3'UTR of each gene was analyzed for potential miRNA binding sites. Identification of targets for viral miRNAs is difficult as many prediction algorithms rely on identification of conservation between human and mouse genomes in predicted target sites in 3'UTRs as an effective way to eliminate false positives. The rhesus lymphocryptovirus has conserved miRNAs with EBV(Cai et al., 2006), however evolutionarily rhesus is so closely related to human that the cellular UTRs are totally conserved and not useful to eliminate potential targets. Due to this limitation, the PITA prediction program was chosen to identify potential BART miRNA target sites in each 3'UTR. PITA uses the difference in free energy between the binding of the miRNA to 3'UTR with the energy needed to disrupt the predicted secondary structure of the 3'UTR in that location (Kertesz et al., 2007). Each BH3-only gene had at least one predicted target site in the 3'UTR of the corresponding mRNA (Table 1). PITA also successfully predicted the miR-BART5 target site identified in the PUMA 3'UTR (Choy et al., 2008). Of the six BH3-only genes identified by the expression arrays, Bim had the largest number and highest scoring target sites.

Bim is a target of multiple BART miRNAs

To identify effects on these potential targets from the microarray analysis, cell lysates of the four AGS cell lines were analyzed by immunoblotting for protein expression of PUMA, Bim, Bik, and BNIPL (Figure 4A). Expression of BNIPL could not be detected with available antibodies (data not shown). The microarray analysis suggested that BNIPL is expressed at an extremely low level, possibly explaining the lack of detection by Western blotting. There are two isoforms of PUMA (α and β) detected by immunoblotting. Although PUMA has been shown to be targeted by miR-BART5, PUMAα was downregulated in the cell lines containing either cluster of miRNAs (Choy et al., 2008). PUMAβ was only slightly decreased in cells expressing the first cluster of miRNAs, despite both isoforms sharing a common 3'UTR (Figure 4A, B). Bik was predicted to be targeted by miR-BART11 in Cluster II, however, the Bik protein level was not reduced by either cluster individually or in combination (Figure 4A).

Importantly, expression of Bim was clearly decreased in the Cluster I cell line and was further decreased in the cell line expressing both clusters. Bim can exist in three alternatively spliced isoforms, Bim_{EL}, Bim_{L}, and Bim_{S}, however, only Bim_{EL} was detected in AGS cells. The Bim_{EL} protein signal was reduced more than two fold in the cell lines that express the Cluster I miRNAs (Figure 4A, B). There are several targets sites predicted in the 3'UTR of Bim for Cluster I miRNAs including miR-BART1-5p, 4, and 5, as well as additional sites for Cluster II miRNAs miR-BART9, 11-3p, 11-5p, 12, and 18-3p (Table 1 and Figure 5A). These data suggest that the combined expression of the miRNAs in Cluster I miRNAs is sufficient to downregulate Bim at the protein level and that the addition of Cluster II miRNAs further decreases its expression.

MicroRNAs have been shown to disrupt protein translation and additionally may decrease the mRNA levels of the target. Bim was identified due to the small mRNA decrease detected by microarray, however, this potential effect on transcription was not detected using quantitative RT-PCR to measure Bim mRNA (Figure 4C). Quantitative PCR was performed with primers specific to the Bim coding sequence, and the dissociation curves revealed specific peaks with the appropriate melting temperature after 20–25 cycles of PCR, indicating this assay was faithfully measuring the levels of Bim mRNA. This finding suggests that the downregulation of Bim occurs primarily post-transcriptionally and is consistent with regulation by miRNAs.

To determine whether the BART miRNAs act via the Bim 3' UTR, reporter assays were developed. The entire 4.2 kb Bim 3' UTR containing the 16 predicted BART miRNA

binding sites was fused to a Renilla luciferase reporter in a single vector that also expresses Firefly luciferase as a transfection control from a separate promoter (Figure 5A). The ratio of expression was determined to identify specific effects on the Bim 3' UTR. The activity regulated by the Bim 3'UTR was decreased by both clusters of miRNAs, suggesting that the Cluster II miRNAs also negatively regulate the Bim 3' UTR (Figure 5B).

To further delineate functional sites in the 3' UTR, the two additional reporter constructs were generated that contained either the first or the second half of the 3'UTR. Each of these constructs contains numerous potential binding sites of the BART miRNAs (Figure 5A). The 5' half contains 8 predicted sites for Cluster I miRNAs and 1 site for miR-BART12 while the 3' half contains sites for 5 miRNAs in Cluster II and 2 sites for miR-BART4 from Cluster I. Surprisingly, Cluster I did not affect either construct while Cluster II slightly decreased activity the 5' half of the UTR reporter (Figure 5B). These data further illustrate the complexity of translational regulation by miRNAs and suggest that binding to the entire UTR by one or multiple miRNAs is required for regulation in this cell line (Figure 5B). It is possible that the complex regulation by multiple miRNAs in part reflects the length of the Bim 3' UTR.

In order to further define the contribution of the individual BART miRNAs in the downregulation of Bim, individual miRNAs were cloned into the pcDNA3 vector. These vectors were designed similarly to the vectors expressing the entire clusters, with smaller pieces of EBV genomic DNA being amplified and cloned into the expression vector. However, in some cases miRNA expression was not detected when using DNA fragments specific for a single miRNA. Cell lines expressing miR-BART1, 3, 5, and 9 were generated and expression was confirmed by RT-PCR (Figure 6A). Expression of miR-BART4, 11 and 12 was not detected in the individual cell lines despite being expressed from similarly sized fragments of DNA. However, it was possible to express these miRNAs by including the adjacent miRNA in the expression vector, so cell lines that express miR-BART4 with miR-BART3 or miR-BART1 and a cell line that expresses miR-BART11 and 12 together were also generated (Figure 6A).

Analysis of the Bim_{EL} protein levels in cells expressing the miRNAs revealed that its expression was affected by several of the individual miRNAs with cell lines expressing miR-BART1, 3, 9, 11 and 12 all having decreased Bim_{EL} levels (Figure 6B and C). The cell lines expressing miR-BART9 and miR-BART11 and 12 had the strongest and most consistent downregulation of Bim, with some decrease detected in miR-BART1 and miR-BART3 expressing cells. Surprisingly, expression of miR-BART1 and 3 together or in combination with miR-BART4 did not appear to have an additive effect in decreasing Bim expression. Notably miR-BART5, which has two predicted target sites in the Bim 3' UTR, did not decrease Bim and Bim expression was consistently higher in the miR-BART5 cell line than in the control. Additionally none of the individual miRNAs, including miR-BART5, decreased the expression of PUMA (Figure 6B). Interestingly in the luciferase reporter assay, the reporter activity of the Bim 3'UTR was not downregulated in any of the individual expressing cell lines (Figure 6D). These findings confirm that multiple miRNAs are required to negatively regulate the full length 3' UTR.

DISCUSSION

In this study, an effect on the inhibition of apoptosis was identified for the EBV BART miRNAs and the data indicate that apoptosis may be targeted through effects on multiple cellular genes. One important target was shown to be the BH3 only, Bcl2 family member Bim, which is predicted to contain multiple miRNA binding sites in the 3'UTR of the Bim message. Bim expression at the protein level was decreased in the Cluster I cell line and in

several cell lines expressing individual miRNAs. Interestingly, both Cluster I or Cluster II could decrease activity in the luciferase reporter assays but this repression required the entire 3'UTR. Additionally, none of the individual miRNAs could decrease reporter activity. This may indicate that the miRNA target sites that are responsible for the decreased endogenous protein level are within the 5' UTR or the coding region of the Bim mRNA and therefore would not be detected by the reporter assay that solely measures the activity against the 3'UTR. Although the data suggest that the BART miRNAs decrease Bim protein, it is also possible that the miRNAs act indirectly to decrease the levels of Bim through effects on positive cellular regulators. However, considering that the clusters of miRNAs affect both the endogenous Bim and a 3'UTR reporter, potential indirect effects might reflect effects on cellular miRNAs that would target the 3'UTR to regulate Bim translation. Future studies on the complex regulation of the Bim 3'UTR should clarify this point.

This study focuses on regulation of apoptosis in response to the chemical compound etoposide. Etoposide is known to induce a p53 dependent cell death in a wide variety of cell lines (Montecucco and Biamonti, 2007; van Maanen et al., 1988). Interestingly, EBV malignancies often show a striking lack of p53 mutations (Edwards and Raab-Traub, 1994; Effert et al., 1992), suggesting that EBV encodes for functions that can inhibit p53 mediated apoptosis to promote carcinogenesis. This study has shown that the BART miRNAs can serve to inhibit apoptosis that is induced through a p53 dependent mechanism. Of note, the inhibition of apoptosis seen in this study was more apparent at 5μM etoposide than at 25μM. The degree to which PARP cleavage and caspase activation occurs in response to etoposide was observed to be concentration dependent. At lower concentrations, and thus less caspase activation, the BART miRNAs were more capable of inhibiting this process, suggesting that the inhibition of apoptosis is incomplete. Perhaps in the context of a full viral infection, other viral factors combine with the BART miRNAs in order to enact a more efficient arrest of apoptosis.

Bim is now the second member of the BH3-only group of the Bcl2 family that has been shown to be a target of the BART miRNAs, in addition to PUMA, and other members of this family may also be targets for BART miRNAs (Choy et al., 2008). Four other family members were also decreased as detected by the microarray analysis and each gene contains potential miRNA target sites in the 3'UTR of their corresponding transcripts. However, decreased Bik was not detected at the protein level and BNIPL is apparently expressed at very low levels in AGS cells given its low intensity on the microarrays, and could not be detected by Western blotting. BNIPL may be a target of the BART miRNAs in cells that express this gene. The two other BH3 only group members were detected by microarray, Hrk and Bcl-G (which exists as two alternatively spliced isoforms, one of which contains only a BH3 domain), have yet to be evaluated. Other prominent members of the BH3 only group of genes include Bad, Bid, and Noxa (Lomonosova and Chinnadurai, 2008). However, effects on expression of Bad or Bid by the BART miRNAs were not detected in the AGS cell line (data not shown).

It is likely that multiple differences between cell lines contribute to different effects of the miRNAs. PUMA was not downregulated by miR-BART5 in the AGS cell lines generated in this study when it was clearly shown to be targeted by Choy *et al*. Potentially different levels of PUMA mRNA in the cell lines used in the two studies likely contribute to regulation by miRNAs. Differences in cellular miRNA expression could also affect the activity of viral miRNAs through their effects on the cellular transcript. Several cellular miRNAs have been identified that regulate the 3'UTR of the Bim transcript. The miR-17-92 cluster of miRNAs, which is highly expressed in several forms of cancer, contains two miRNAs that target Bim, miR-19 and miR-92 (Ventura et al., 2008). miR-25, a member of the miR-106b-25 cluster, also represses Bim in a gastric cancer cell line (Petrocca et al., 2008). Additionally, miR-221

and miR-222 that are induced by activation of the ERK-MAPK pathway also decrease Bim (Terasawa et al., 2009).

It has been previously shown that Bim is decreased during latent EBV infection of B lymphocytes as infection of EBV negative Burkitt's lymphoma cell lines with EBV leads to posttranscriptional downregulation of Bim which is dependent upon the ERK-MAPK pathway (Clybouw et al., 2005). The ERK-MAPK pathway is thought to downregulate Bim through phosphorylation and subsequent ubiquitin mediated degradation (Ley et al., 2003; Luciano et al., 2003; Mouhamad et al., 2004). EBV LMP1 activates the ERK signaling pathway and thus could contribute to this decrease of Bim in lymphocytes (Liu et al., 2003; Mainou, Everly, and Raab-Traub, 2007). Interestingly, in transformed lymphocytes where the BART miRNAs are not expressed, the EBV latent proteins EBNA3A and EBNA3C also decrease Bim transcription (Anderton et al., 2008) through an epigenetic mechanism involving methylation of the Bim promoter (Paschos et al., 2009). Perhaps the BART miRNAs replace some of the EBNA functions during different forms of latency. The fact that the virus has evolved multiple mechanisms to inhibit Bim suggests that the prevention of Bim mediated apoptosis is critical for the viral life cycle.

MATERIALS AND METHODS

Cell Culture and Constructs

The gastric carcinoma cell line AGS was grown in F-12 media (Gibco) with 10% fetal bovine serum and antibiotic/antimycotic (Gibco). Stable cell lines expressing miRNAs were generated by transfection of pcDNA3 constructs and selection in media containing 500 μg/ml G418 (Gibco) and 400 μg/ml zeocin (Invitrogen) as required.

The pcDNA3 miRNA constructs were generated by PCR amplification of the miRNA containing fragments from genomic EBV DNA followed by insertion into the BamHI/EcoRI sites of pcDNA3.1 neo (Cluster I) or pcDNA3.1 zeo (Cluster II). The primers used for Cluster I amplification were G1 (TTTGGATCCCGGAATATGCAAGTGCATCTT) and G2 (TTTGAATTCTAGAGGCTCTCCCAACACAAT), which generates a 1413 base pair fragment containing the Cluster I miRNAs; and G9 (TATAGATCTATCCTTCTTCGGTAGGGAG) and G6 (TATGAATTCAAGGAAAGGCCTGCTGTCAT), which generates a 3185 base pair fragment containing the Cluster II miRNAs. The Cluster II fragment does not contain miR-BART21 which was identified subsequent to the beginning of this study (Zhu et al., 2009). The individual miRNAs were cloned as fragments of approximately 250 base pairs in size, and inserted into pcDNA3.1 zeo. The primers used for amplification were as follows: 5'BART1 (TTTAAGCTTCTACTTGCCTCGGCATCTC) and 3'BART1 (TTGGATCCGGTGGGGTCGTGACTATAT) for miR-BART1; 5'BART3 (TTTAAGCTTCTCCTTGTCTTGATAATCCCTG) and 3'BART3 (TTGGATCCCCCCCCCGTATAGATTT) for miR-BART3; 5'BART3 and 3'BART4 (TTGGATCCGTTTGTTAACCCCTTCTCCGG) for miR-BART3-4; 5'BART3 and 3'BART1 for miR-BART3-4-1; 5'BART4 (TTTAAGCTTGCCTCAGTGCCACTTTTACC) and 3'BART1 for miR-BART4-1; 5'BART5 (TTTAAGCTTTCTGTTAACCAGGTCAGTGG) and 3'BART5 (TTGGATCCGTTTATCAATTGTGGGATATGG) for miR-BART5; 5'BART9 (TTTAAGCTTTGGGTGGTGCTATGGGCTCC) and 3'BART9 (TTGGATCCCCTCACGTTGGCCAGGAAAGGG) for miR-BART9; and 5'BART11 (TTTAAGCTTACACCTTTGAGGACAC) and 3'BART12 (TTGGATCCTAACACATAAGCGCACAAGCGG) for miR-BART11-12.

The Bim reporter constructs were made amplifying the Bim 3'UTR from human genomic DNA and cloning into the XhoI/NotI sites in between the Renilla luciferase coding sequence and the poly(A) site of psiCHECK-2 (Promega). The primers used for the amplification were 5'BimFL (TTTTGTCGACCAGGTTCTTTGCGGAGCC) and 3'BimFL (TTTTGCGGCCGCATTGCACAAGTAAAGTGGCAATTA). The two half UTR reporters were generated by cutting the full length plasmid with XhoI (which cleaves at an internal site in the UTR approximately in the middle) and NotI to generate a fragment that contains the second half of the UTR. This fragment was recloned into an empty psiCHECK-2 vector while the first half vector was generated by a blunt ligation of the remaining vector after the second half was removed.

Western Blot analysis

Protein lysates were prepared from cells and Western blot analysis was performed as previously described (Mainou, Everly, and Raab-Traub, 2005). Primary antibodies used were rabbit α-PARP (Cell Signaling, 9542), rabbit α-Bim (Cell Signaling, 2819), rabbit α-PUMA (Cell Signaling, 4976), rabbit α-Bik (Cell Signaling, 4592), rabbit α-Caspase-3 (Abcam, ab47131) and goat α-GRP78 (Santa Cruz, C-20). For etoposide treatment experiments, cells were grown to 75% confluency, and then treated with indicated amount of etoposide for 24 hours followed by harvesting the cells for Western blotting procedure.

Northern Blot analysis and quantitative RT-PCR

Total cellular RNA was prepared from cells using TRIzol reagent (Invitrogen) as was previously described (Edwards, Marquitz, and Raab-Traub, 2008). Northern Blots for miR-BART4 and miR-BART9 were performed as previously described (Edwards, Marquitz, and Raab-Traub, 2008). Quantitative RT-PCR was performed for the BART miRNAs using the miScript system (Qiagen) according to manufacturer's instructions. Briefly, miRNAs are polyadenylated and then reversed transcribed using an oligo-dT primer that contains a universal tag at the 5' end. A subsequent PCR step is then performed using a primer that corresponds to the universal tag and a primer that is specific for each miRNA (primers are specifically designed by Qiagen, the sequences of which are not made available to the consumer). PCR product accumulation is monitored by the addition of SYBR green dye. The cycle threshold (C_T) was determined as the number of PCR cycles required for a given reaction to reach an arbitrary fluorescence value within the linear amplification range. The change in C_T (ΔC_T) was determined between each individual miRNA compared to the C_T observed from C666 cells, and the change in ΔCT ($\Delta\Delta C_T$) was determined by adjusting for the difference in a control reaction, which amplifies the U5A small nuclear RNA. The expression relative to C666 cells was determined as $2^{\Delta\Delta CT}$ since each PCR cycle results in a twofold amplification of each PCR product.

Quantitative RT-PCR for Bim mRNA levels was performed using a Quantitect SYBR green reverse transcription-PCR kit and has previously described (Kung and Raab-Traub, 2008). The Primers used were 5'BimELqRT (GCTGTCTCGATCCTCCAGTG) and 3'BimELqRT (GTTAAACTCGTCTCCAATACG). The ΔC_T for Bim was determined in a similar manner in comparison to the levels in the pcDNA3 control cells and the $\Delta\Delta C_T$ was calculated using a reaction amplifying GAPDH as a control reaction. The primers used to amplify GAPDH were qGAPDH5' (TGCACCACCAACTGCTTAGC) and qGAPDH3' (GAGGGGCCATCCACAGTCTT). Again, the expression relative to control cells was determined as $2^{\Delta\Delta CT}$.

Microarray analysis

Total RNA was prepared using the RNeasy Plus Mini Kit (Qiagen) from AGS cells expressing Cluster I and Cluster II as well as double negative pcDNA3 controls. RNA was

then amplified and hybridized to a dual color 4×44K whole Human genome microarray (Agilent) by the UNC Lineberger Comprehensive Cancer Center Genomics and Bioinformatics Core Facility. Microarrays were scanned using an Axon 4200 Scanner (Molecular Devices) and normalized using GenePix 5.0 software. Normalized data was uploaded into the University of North Carolina Microarray Database and is available for public download at http://genome.unc.edu. Normalized data was also analyzed using Genespring GX software (Agilent). Genes that showed decreased expression in miRNA expressing cells compared to controls in all four arrays were considered in further analysis. Downregulated genes were narrowed down by selecting only those that contained reference to involvement in apoptosis according the Gene Ontology annotations in Genespring GX. A table containing the expression data for the 133 genes that met this criterion is contained in the supplementary materials (Supplementary Table 1). Potential miRNA target sites within the 3'UTR of these genes were identified using the publicly available PITA software (Kertesz et al., 2007). ΔΔG scores of −9.00 or lower were considered to be potential miRNA target sites (Supplementary Table 2).

Luciferase Assays

Stable miRNA expressing AGS cells and controls were grown to 75% confluency in 6 well plates. The cells were then transfected with 250 ng of reporter with Lipofectamine 2000 (Invitrogen) according the manufacturer's instructions. After 24 hours the transfection reagent was removed and replaced with fresh media. At 48 hours after transfection cells were harvested and assayed using a Dual-Luciferase Reporter Assay System (Promega) according to manufacturer's instructions. Luciferase activity values were obtained using an LMax Luminometer (Molecular Devices). Renilla luciferase activity was first normalized to the control Firefly luciferase activity and then normalized to the empty reporter construct.

Supplementary Material

Refer to Web version on PubMed Central for supplementary material.

Acknowledgments

A.R.M. is supported by fellowship 5059-08 from the Leukemia and Lymphoma Society. This study was supported by grant CA138811 from the National Institutes of Health to N.R.T.

References

Amoroso R, Fitzsimmons L, Thomas WA, Kelly GL, Rowe M, Bell AI. Quantitative studies of Epstein-Barr virus-encoded miRNAs provide novel insights into their regulation. J Virol.

Anderton E, Yee J, Smith P, Crook T, White RE, Allday MJ. Two Epstein-Barr virus (EBV) oncoproteins cooperate to repress expression of the proapoptotic tumour-suppressor Bim: clues to the pathogenesis of Burkitt's lymphoma. Oncogene. 2008; 27(4):421–33. [PubMed: 17653091]

Barranco SC, Townsend CM Jr, Casartelli C, Macik BG, Burger NL, Boerwinkle WR, Gourley WK. Establishment and characterization of an in vitro model system for human adenocarcinoma of the stomach. Cancer Res. 1983; 43(4):1703–9. [PubMed: 6831414]

Bartel DP. MicroRNAs: genomics, biogenesis, mechanism, and function. Cell. 2004; 116(2):281–97. [PubMed: 14744438]

Barth S, Pfuhl T, Mamiani A, Ehses C, Roemer K, Kremmer E, Jaker C, Hock J, Meister G, Grasser FA. Epstein-Barr virus-encoded microRNA miR-BART2 down-regulates the viral DNA polymerase BALF5. Nucleic Acids Res. 2008; 36(2):666–75. [PubMed: 18073197]

Cai X, Schafer A, Lu S, Bilello JP, Desrosiers RC, Edwards R, Raab-Traub N, Cullen BR. Epstein-Barr virus microRNAs are evolutionarily conserved and differentially expressed. PLoS Pathog. 2006; 2(3):e23. [PubMed: 16557291]

Cheung ST, Huang DP, Hui AB, Lo KW, Ko CW, Tsang YS, Wong N, Whitney BM, Lee JC. Nasopharyngeal carcinoma cell line (C666-1) consistently harbouring Epstein-Barr virus. Int J Cancer. 1999; 83(1):121–6. [PubMed: 10449618]

Choy EY, Siu KL, Kok KH, Lung RW, Tsang CM, To KF, Kwong DL, Tsao SW, Jin DY. An Epstein-Barr virus-encoded microRNA targets PUMA to promote host cell survival. J Exp Med. 2008; 205(11):2551–60. [PubMed: 18838543]

Clybouw C, McHichi B, Mouhamad S, Auffredou MT, Bourgeade MF, Sharma S, Leca G, Vazquez A. EBV infection of human B lymphocytes leads to down-regulation of Bim expression: relationship to resistance to apoptosis. J Immunol. 2005; 175(5):2968–73. [PubMed: 16116183]

Cosmopoulos K, Pegtel M, Hawkins J, Moffett H, Novina C, Middeldorp J, Thorley-Lawson DA. Comprehensive profiling of Epstein-Barr virus microRNAs in nasopharyngeal carcinoma. J Virol. 2009; 83(5):2357–67. [PubMed: 19091858]

Cullen BR. Viruses and microRNAs. Nat Genet. 2006; 38(Suppl):S25–30. [PubMed: 16736021]

Edwards RH, Marquitz AR, Raab-Traub N. Epstein-Barr virus BART microRNAs are produced from a large intron prior to splicing. J Virol. 2008; 82(18):9094–106. [PubMed: 18614630]

Edwards RH, Raab-Traub N. Alterations of the p53 gene in Epstein-Barr virus-associated immunodeficiency-related lymphomas. J Virol. 1994; 68(3):1309–15. [PubMed: 8107196]

Effert P, McCoy R, Abdel-Hamid M, Flynn K, Zhang Q, Busson P, Tursz T, Liu E, Raab-Traub N. Alterations of the p53 gene in nasopharyngeal carcinoma. J Virol. 1992; 66(6):3768–75. [PubMed: 1349927]

Fukayama M, Hino R, Uozaki H. Epstein-Barr virus and gastric carcinoma: virus-host interactions leading to carcinoma. Cancer Sci. 2008; 99(9):1726–33. [PubMed: 18616681]

Gilligan K, Sato H, Rajadurai P, Busson P, Young L, Rickinson A, Tursz T, Raab-Traub N. Novel transcription from the Epstein-Barr virus terminal EcoRI fragment, DIJhet, in a nasopharyngeal carcinoma. J Virol. 1990; 64(10):4948–56. [PubMed: 2168978]

Gottwein E, Mukherjee N, Sachse C, Frenzel C, Majoros WH, Chi JT, Braich R, Manoharan M, Soutschek J, Ohler U, Cullen BR. A viral microRNA functions as an orthologue of cellular miR-155. Nature. 2007; 450(7172):1096–9. [PubMed: 18075594]

Grundhoff A, Sullivan CS, Ganem D. A combined computational and microarray-based approach identifies novel microRNAs encoded by human gamma-herpesviruses. Rna. 2006; 12(5):733–50. [PubMed: 16540699]

Guo H, Ingolia NT, Weissman JS, Bartel DP. Mammalian microRNAs predominantly act to decrease target mRNA levels. Nature. 2010; 466(7308):835–40. [PubMed: 20703300]

Hitt MM, Allday MJ, Hara T, Karran L, Jones MD, Busson P, Tursz T, Ernberg I, Griffin BE. EBV gene expression in an NPC-related tumour. Embo J. 1989; 8(9):2639–51. [PubMed: 2479554]

Kassis J, Maeda A, Teramoto N, Takada K, Wu C, Klein G, Wells A. EBV-expressing AGS gastric carcinoma cell sublines present increased motility and invasiveness. Int J Cancer. 2002; 99(5): 644–51. [PubMed: 12115496]

Kertesz M, Iovino N, Unnerstall U, Gaul U, Segal E. The role of site accessibility in microRNA target recognition. Nat Genet. 2007; 39(10):1278–84. [PubMed: 17893677]

Kim do N, Chae HS, Oh ST, Kang JH, Park CH, Park WS, Takada K, Lee JM, Lee WK, Lee SK. Expression of viral microRNAs in Epstein-Barr virus-associated gastric carcinoma. J Virol. 2007; 81(2):1033–6. [PubMed: 17079300]

Kung CP, Raab-Traub N. Epstein-Barr virus latent membrane protein 1 induces expression of the epidermal growth factor receptor through effects on Bcl-3 and STAT3. J Virol. 2008; 82 (11): 5486–93. [PubMed: 18367518]

Ley R, Balmanno K, Hadfield K, Weston C, Cook SJ. Activation of the ERK1/2 signaling pathway promotes phosphorylation and proteasome-dependent degradation of the BH3-only protein, Bim. J Biol Chem. 2003; 278(21):18811–6. [PubMed: 12646560]

Lim LP, Lau NC, Garrett-Engele P, Grimson A, Schelter JM, Castle J, Bartel DP, Linsley PS, Johnson JM. Microarray analysis shows that some microRNAs downregulate large numbers of target mRNAs. Nature. 2005; 433(7027):769–73. [PubMed: 15685193]

Liu LT, Peng JP, Chang HC, Hung WC. RECK is a target of Epstein-Barr virus latent membrane protein 1. Oncogene. 2003; 22(51):8263–70. [PubMed: 14614450]

Lo AK, To KF, Lo KW, Lung RW, Hui JW, Liao G, Hayward SD. Modulation of LMP1 protein expression by EBV-encoded microRNAs. Proc Natl Acad Sci U S A. 2007; 104(41):16164–9. [PubMed: 17911266]

Lomonosova E, Chinnadurai G. BH3-only proteins in apoptosis and beyond: an overview. Oncogene. 2008; 27(Suppl 1):S2–19. [PubMed: 19641503]

Luciano F, Jacquel A, Colosetti P, Herrant M, Cagnol S, Pages G, Auberger P. Phosphorylation of Bim-EL by Erk1/2 on serine 69 promotes its degradation via the proteasome pathway and regulates its proapoptotic function. Oncogene. 2003; 22(43):6785–93. [PubMed: 14555991]

Lung RW, Tong JH, Sung YM, Leung PS, Ng DC, Chau SL, Chan AW, Ng EK, Lo KW, To KF. Modulation of LMP2A expression by a newly identified Epstein-Barr virus-encoded microRNA miR-BART22. Neoplasia. 2009; 11(11):1174–84. [PubMed: 19881953]

Mainou BA, Everly DN Jr, Raab-Traub N. Epstein-Barr virus latent membrane protein 1 CTAR1 mediates rodent and human fibroblast transformation through activation of PI3K. Oncogene. 2005; 24(46):6917–24. [PubMed: 16007144]

Mainou BA, Everly DN Jr, Raab-Traub N. Unique signaling properties of CTAR1 in LMP1-mediated transformation. J Virol. 2007; 81(18):9680–92. [PubMed: 17626074]

Montecucco A, Biamonti G. Cellular response to etoposide treatment. Cancer Lett. 2007; 252(1):9–18. [PubMed: 17166655]

Mouhamad S, Besnault L, Auffredou MT, Leprince C, Bourgeade MF, Leca G, Vazquez A. B cell receptor-mediated apoptosis of human lymphocytes is associated with a new regulatory pathway of Bim isoform expression. J Immunol. 2004; 172(4):2084–91. [PubMed: 14764673]

Nachmani D, Stern-Ginossar N, Sarid R, Mandelboim O. Diverse herpesvirus microRNAs target the stress-induced immune ligand MICB to escape recognition by natural killer cells. Cell Host Microbe. 2009; 5(4):376–85. [PubMed: 19380116]

Paschos K, Smith P, Anderton E, Middeldorp JM, White RE, Allday MJ. Epstein-barr virus latency in B cells leads to epigenetic repression and CpG methylation of the tumour suppressor gene Bim. PLoS Pathog. 2009; 5(6):e1000492. [PubMed: 19557159]

Petrocca F, Visone R, Onelli MR, Shah MH, Nicoloso MS, de Martino I, Iliopoulos D, Pilozzi E, Liu CG, Negrini M, Cavazzini L, Volinia S, Alder H, Ruco LP, Baldassarre G, Croce CM, Vecchione A. E2F1-regulated microRNAs impair TGFbeta-dependent cell-cycle arrest and apoptosis in gastric cancer. Cancer Cell. 2008; 13(3):272–86. [PubMed: 18328430]

Pfeffer S, Zavolan M, Grasser FA, Chien M, Russo JJ, Ju J, John B, Enright AJ, Marks D, Sander C, Tuschl T. Identification of virus-encoded microRNAs. Science. 2004; 304(5671):734–6. [PubMed: 15118162]

Pratt ZL, Kuzembayeva M, Sengupta S, Sugden B. The microRNAs of Epstein-Barr Virus are expressed at dramatically differing levels among cell lines. Virology. 2009; 386(2):387–97. [PubMed: 19217135]

Raab-Traub N. Epstein-Barr virus in the pathogenesis of NPC. Semin Cancer Biol. 2002; 12(6):431–41. [PubMed: 12450729]

Rickinson, AB.; Kieff, E. Epstein-Barr Virus. In: Knipe, DM.; Howley, PM., editors. Field's Virology. 4. Lippincott/Williams & Wilkins; Philadelphia, PA: 2001. p. 2575-2627.

Samols MA, Skalsky RL, Maldonado AM, Riva A, Lopez MC, Baker HV, Renne R. Identification of cellular genes targeted by KSHV-encoded microRNAs. PLoS Pathog. 2007; 3 (5):e65. [PubMed: 17500590]

Terasawa K, Ichimura A, Sato F, Shimizu K, Tsujimoto G. Sustained activation of ERK1/2 by NGF induces microRNA-221 and 222 in PC12 cells. Febs J. 2009; 276(12):3269–76. [PubMed: 19438724]

Umbach JL, Kramer MF, Jurak I, Karnowski HW, Coen DM, Cullen BR. MicroRNAs expressed by herpes simplex virus 1 during latent infection regulate viral mRNAs. Nature. 2008; 454(7205): 780–3. [PubMed: 18596690]

van Maanen JM, Retel J, de Vries J, Pinedo HM. Mechanism of action of antitumor drug etoposide: a review. J Natl Cancer Inst. 1988; 80(19):1526–33. [PubMed: 2848132]

Ventura A, Young AG, Winslow MM, Lintault L, Meissner A, Erkeland SJ, Newman J, Bronson RT, Crowley D, Stone JR, Jaenisch R, Sharp PA, Jacks T. Targeted deletion reveals essential and

overlapping functions of the miR-17 through 92 family of miRNA clusters. Cell. 2008; 132(5): 875–86. [PubMed: 18329372]

Xia T, O'Hara A, Araujo I, Barreto J, Carvalho E, Sapucaia JB, Ramos JC, Luz E, Pedroso C, Manrique M, Toomey NL, Brites C, Dittmer DP, Harrington WJ Jr. EBV microRNAs in primary lymphomas and targeting of CXCL-11 by ebv-mir-BHRF1-3. Cancer Res. 2008; 68(5):1436–42. [PubMed: 18316607]

Young LS, Murray PG. Epstein-Barr virus and oncogenesis: from latent genes to tumours. Oncogene. 2003; 22(33):5108–21. [PubMed: 12910248]

Zhu JY, Pfuhl T, Motsch N, Barth S, Nicholls J, Grasser F, Meister G. Identification of novel Epstein-Barr virus microRNA genes from nasopharyngeal carcinomas. J Virol. 2009; 83(7):3333–41. [PubMed: 19144710]

Ziegelbauer JM, Sullivan CS, Ganem D. Tandem array-based expression screens identify host mRNA targets of virus-encoded microRNAs. Nat Genet. 2009; 41(1):130–4. [PubMed: 19098914]

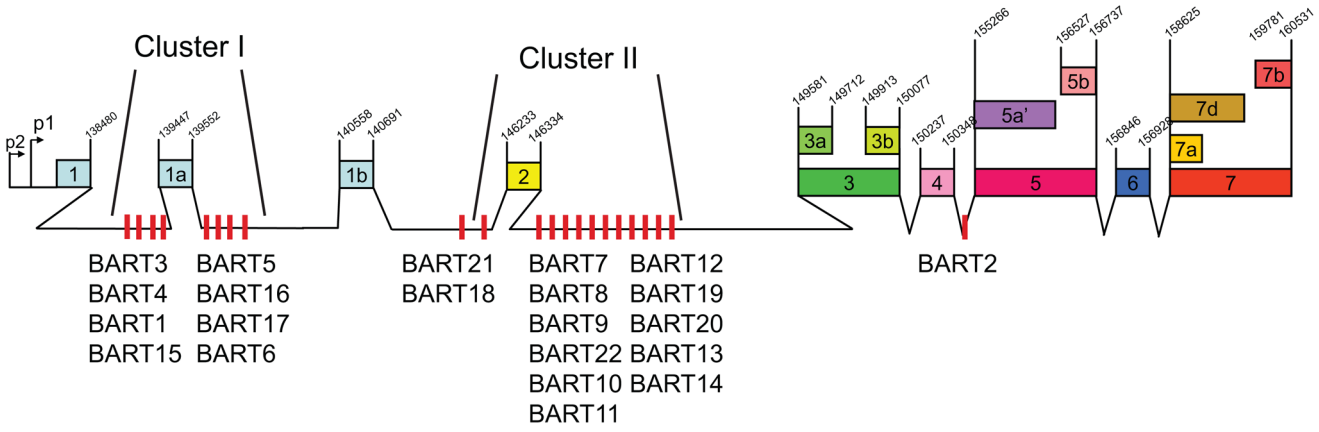

Figure 1. The structure of the EBV BARTs

The EBV BART miRNAs are expressed from the first two introns of the BART RNAs. In order to express these miRNAs exogenenously, the DNA sequences spanning the miRNAs was cloned as two clusters into pcDNA3 expression vectors. Cluster I contains eight miRNAs from the first intron. Cluster II contains 11 miRNAs from the second intron as well as miR-BART18 which is just upstream of exon 2. miR-BART2, which is contained in the intron between exons 4 and 5, and miR-BART21, which is upstream of miR-BART18 were not included in this study.

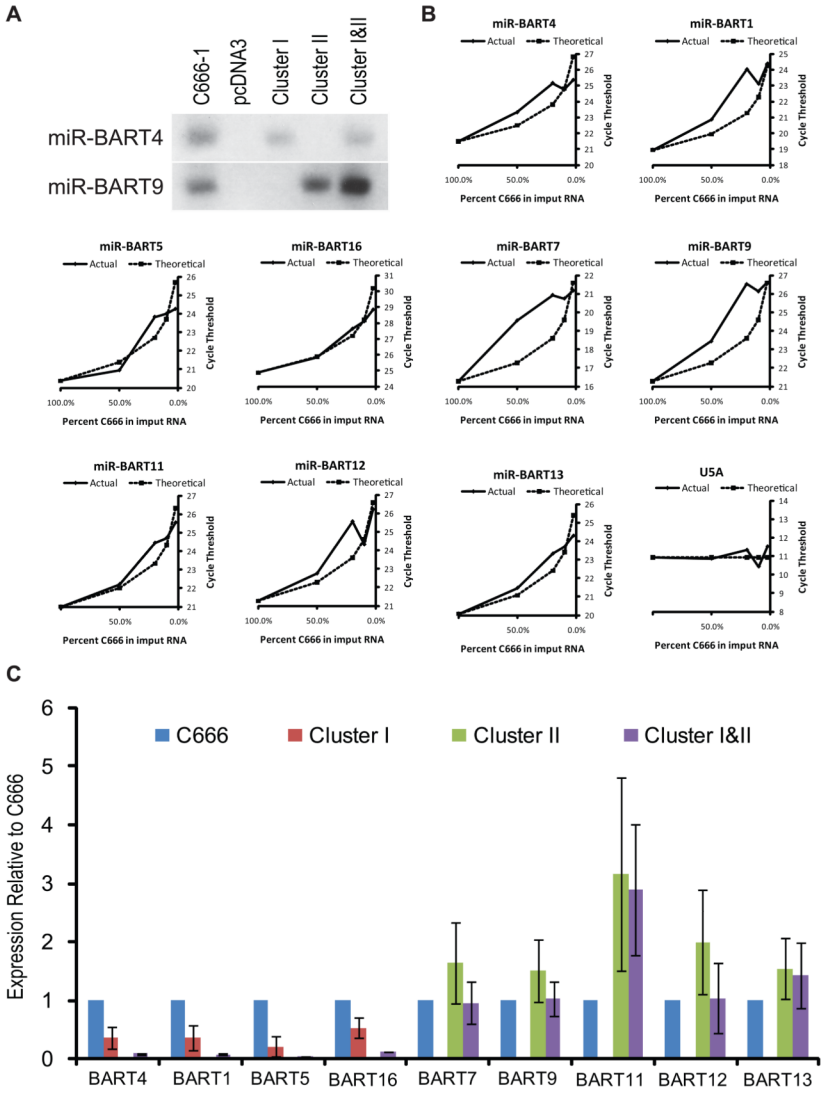

Figure 2. Generation of stable cell lines that express the BART miRNAs

AGS cells were transfected with two pcDNA3 vectors containing Cluster I or Cluster II as well as appropriate controls to generate four stable cell lines: Cluster I and Cluster II expressed together, Cluster I and II by themselves each with a control vector, and a double control vector line. **A.** Northern blot analysis of total RNA from the four cell lines for a miRNA representative of each cluster. RNA from the EBV infected NPC cell line, C666-1, was used as a positive control for expression. **B.** Quantitative RT-PCR for the miRNAs listed above each graph. C666-1 RNA was diluted with AGS RNA that lacks BART miRNAs to 50%, 20%, 10%, and 4% of the total input RNA. For each miRNA the actual cycle thresholds obtained are plotted against the theoretical cycle thresholds expected for each dilution. As a control, qRT-PCR was also performed for the small nuclear RNA U5A, which would not be expected to differ in abundance between the C666-1 and AGS cell lines. **C.** Quantitative RT-PCR of the AGS cell lines. RNA from the four stable cell lines was assayed for the abundance of mature miRNAs using the same qRT-PCR system. Graphed is the mean relative abundance of each miRNA in each cell line compared to control C666-1 cells for three independent measurements. Error bars represent the standard error of the mean.

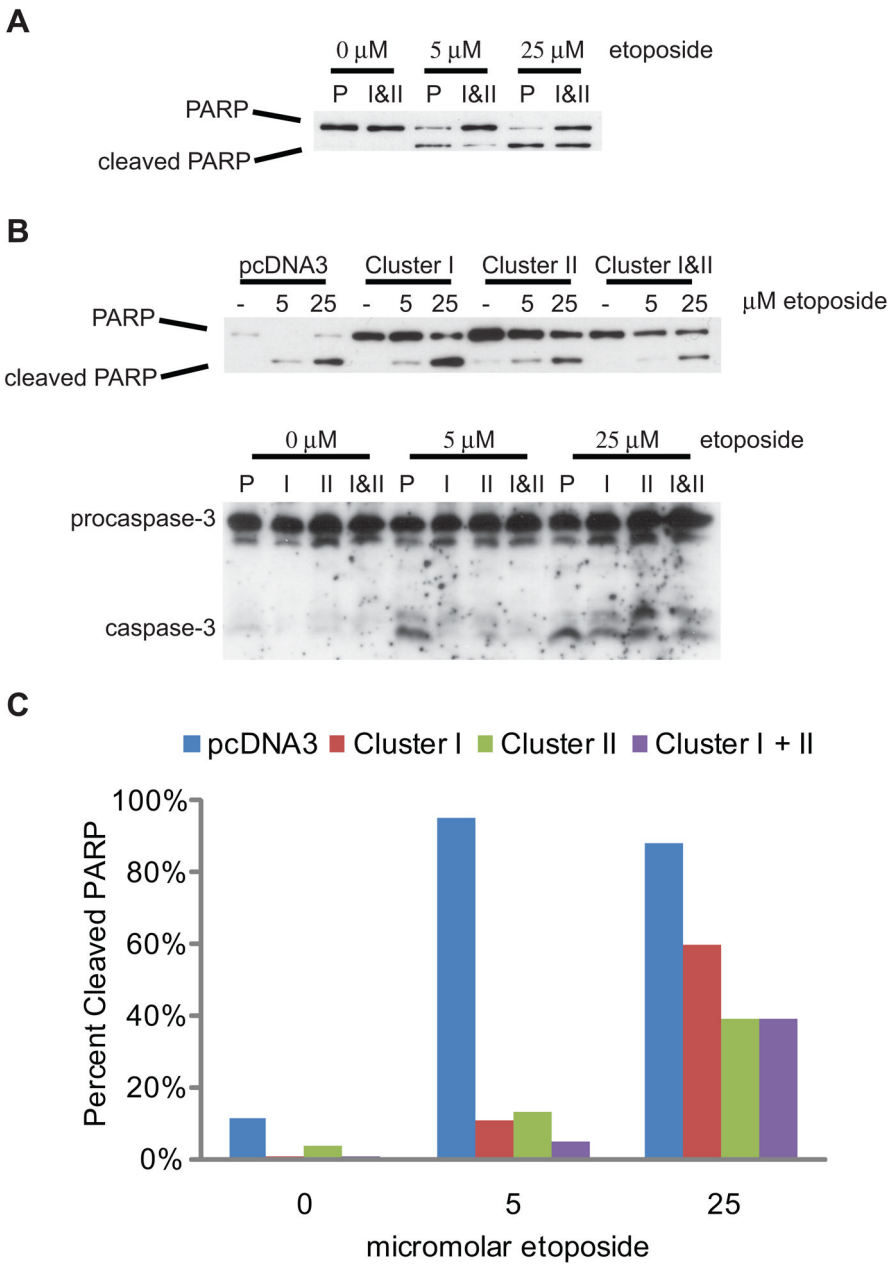

Figure 3. Treatment of AGS cell with etoposide

The AGS stable cell lines were grown in culture in the presence of 5 or 25 μM etoposide for 24 hours. **A.** Control and cells expressing both clusters of miRNAs were harvested and assayed for the induction of apoptosis by assessing the amount of cleaved PARP, a caspase 3 substrate. Protein lysates were run on a SDS-PAGE gel and analyzed for cleaved PARP by Western blotting. **B**. Cells from all four cell lines were harvested and assessed for cleaved PARP as in A (top panel). Lysates from the experiment shown were also run on a separate gel and probed with an antibody that recognizes both the pro- and mature form of caspase-3 (bottom panel). **C.** PARP western blot in B was analyzed by densitometry using Image J software. The percentage of total PARP that is cleaved for each cell line and each treatment condition is presented.

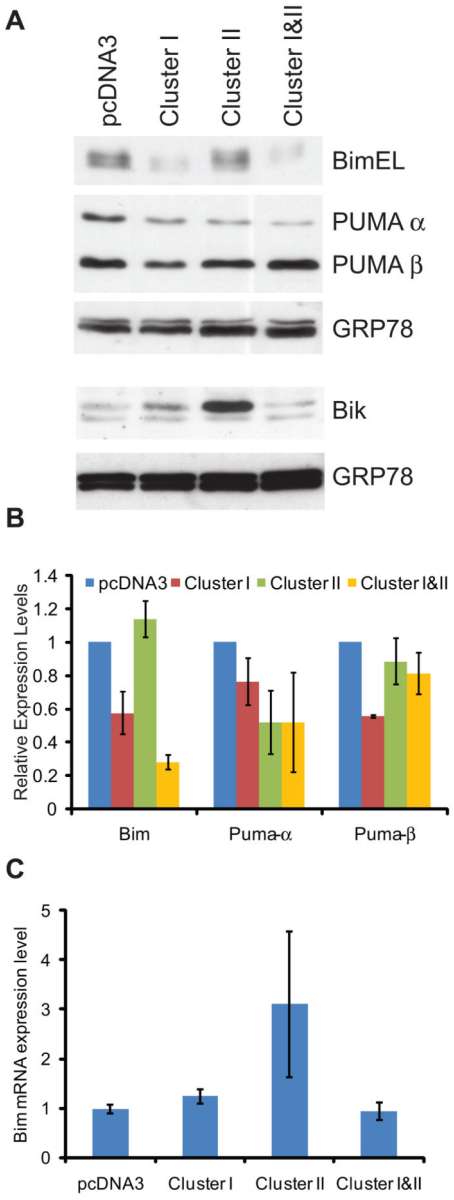

Figure 4. Regulation of BH3-only proteins in AGS cells expressing miRNA clusters

A. Western blot analysis of AGS stable cell lines. Protein lysates were analyzed for expression of Bim_{EL}, PUMAα+β, and Bik. In each case, GRP78 was used as a loading control. **B.** Immunoblots for Bim_{EL} and PUMAα+β were quantitated by densitometry using Image J software. Expression levels were normalized to GRP78 loading control. Plotted is the mean of three independent experiments with error bars representing the standard error of the mean. **C.** Total RNA was prepared from each of the four stable AGS cell lines and qRT-PCR for Bim mRNA was performed. The mean expression level relative to the pcDNA3 control cells in three independent experiments is presented graphically. Error bars represent standard error of the mean.

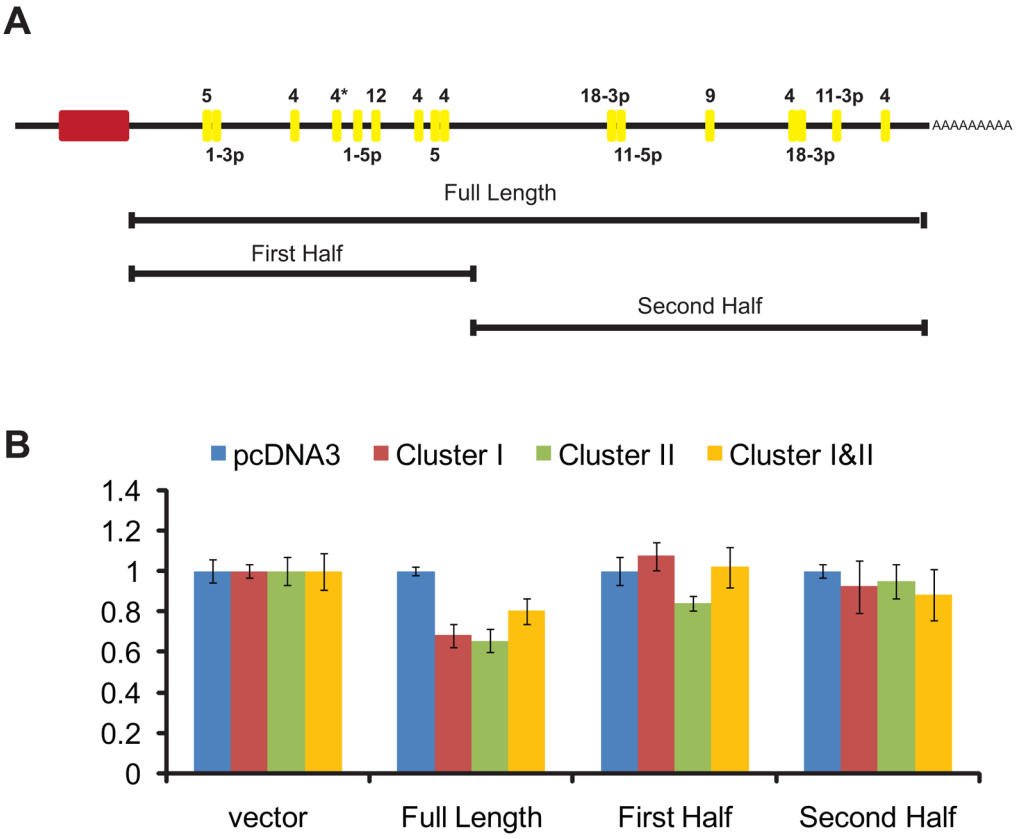

Figure 5. Effects mediated through the Bim 3'UTR

A. A diagram of the Bim mRNA drawn to scale. The green box represents the coding region of the message. Potential miRNA binding sites predicted by PITA are indicated at their relative positions in the 3'UTR. Fragments of the message cloned into reporter vectors are indicated below. **B.** The indicated luciferase reporter vectors were transfected into AGS stable cells and assayed for luciferase activity after 48 hours. Each value represents the ratio of Renilla luciferase/control Firefly luciferase normalized to the control vector in each individual cell line. Plotted is the mean of at least six independent experiments. Error bars represent standard error of the mean.

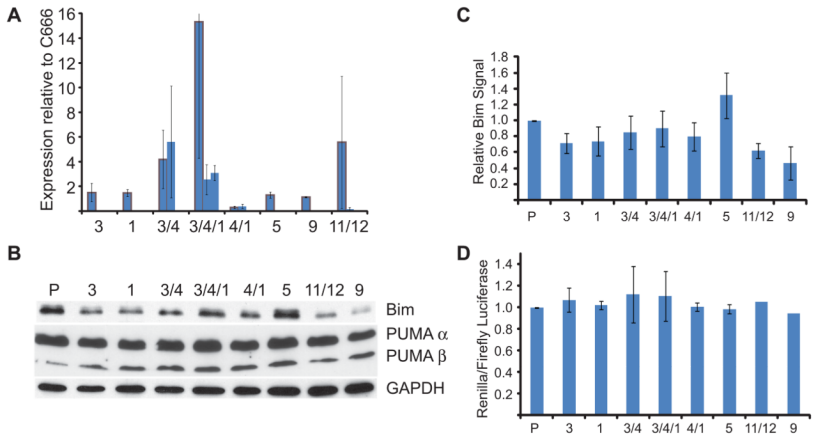

Figure 6. Regulation of Bim in single miRNA expressing cells

A. Expression levels for the AGS stable cell lines expressing individual miRNAs by quantitative RT-PCR. RNA from each of the stable cell lines listed was assayed for the abundance of mature miRNAs using qRT-PCR. For cell lines that express multiple miRNAs, each bar represents expression of a different miRNA, in the order listed on the x axis of the graph. The relative abundance of each miRNA in each cell line compared to control C666-1 cells from three independent experiments is graphed. **B.** Western blot analysis of AGS cell lines expressing single miRNAs. Protein lysates were probed for expression of Bim_{EL}, PUMAα+β, and GAPDH as a loading control. **C.** Immunoblots for Bim_{EL} were analyzed by densitometry using Image J software. The relative signals were normalized to GAPDH loading control. Plotted is the mean of six independent experiments. Error bars represent standard error of the mean. **D.** Luciferase reporter vectors were transfected into AGS stable cells indicated and assayed for luciferase activity after 48 hours. Each value represents the ratio of Renilla luciferase/control Firefly luciferase normalized to the control vector in each individual cell line. Plotted is the mean of two independent experiments. Error bars represent standard error of the mean.

Table 1

PITA predictions of BH3 only family members

Gene	microRNA	Position[a]	Seed[b]	ΔGduplex	ΔGopen	ΔΔG
Bim	miR-BART12	1247	8:1:1	−23.50	−7.17	−16.32
Bim	miR-BART1-5p	1188	8:1:1	−16.50	−3.58	−12.91
Bim	miR-BART4	1040	8:0:0	−26.70	−14.01	−12.68
Bim	miR-BART4	3973	8:0:0	−19.03	−7.32	−11.70
Bim	miR-BART18-3p	3611	8:0:1	−21.50	−10.14	−11.35
Bim	miR-BART11-5p	2686	8:1:0	−17.60	−6.55	−11.04
Bim	miR-BART5	1622	8:1:0	−17.80	−6.85	−10.94
Bim	miR-BART4	3575	8:1:1	−16.30	−5.69	−10.60
Bim	miR-BART4	1449	8:1:1	−17.91	−7.55	−10.35
Bim	miR-BART4	880	8:1:1	−18.60	−8.82	−9.77
Bim	miR-BART9	3085	8:1:0	−19.31	−9.55	−9.75
Bim	miR-BART4	1635	8:1:1	−18.31	−8.57	−9.73
Bim	miR-BART5	313	8:1:0	−16.10	−6.50	−9.59
Bim	miR-BART11-3p	3756	8:1:1	−22.90	−13.42	−9.47
Bim	miR-BART1-5p	320	8:1:1	−16.40	−7.07	−9.32
Bim	miR-BART18-3p	2573	8:0:1	−16.20	−7.09	−9.10
Bcl-G	miR-BART20-5p	18	8:1:1	−18.30	−4.26	−14.03
Bcl-G	miR-BART4	393	8:1:0	−19.00	−6.44	−12.55
Bcl-G	miR-BART12	139	8:1:1	−19.28	−8.19	−11.08
Bcl-G	miR-BART11-5p	16	8:1:0	−15.30	−4.27	−11.02
Bcl-G	miR-BART10	158	8:1:1	−22.20	−11.44	−10.75
Bcl-G	miR-BART20-3p	913	8:1:1	−23.00	−12.49	−10.50
Bcl-G	miR-BART4	1046	8:1:1	−16.90	−6.42	−10.47
Bcl-G	miR-BART15	1073	8:1:1	−12.84	−3.02	−9.81
Bcl-G	miR-BART5	834	8:1:0	−17.40	−8.29	−9.10
Bik	miR-BART11-5p	84	8:1:1	−15.71	−4.66	−11.04
HRK	miR-BART16	268	8:1:0	−18.76	−5.40	−13.35
HRK	miR-BART4	51	8:1:0	−20.91	−9.55	−11.35

Gene	microRNA	Position[a]	Seed[b]	ΔGduplex	ΔGopen	ΔΔG
HRK	miR-BART16	252	8:1:1	−18.40	−8.31	−10.08
BNIPL	miR-BART20-5p	792	8:0:1	−18.95	−6.55	−12.39
BNIPL	miR-BART15	761	8:1:1	−16.92	−4.54	−12.37
BNIPL	miR-BART6-3p	89	8:1:1	−14.40	−3.76	−10.63
BNIPL	miR-BART5	624	8:0:1	−18.40	−8.08	−10.31
PUMA	miR-BART5	485	8:1:0	−26.10	−13.12	−12.97
PUMA	miR-BART20-3p	488	8:1:0	−19.70	−10.34	−9.35
PUMA	miR-BART19-5p	736	8:1:1	−19.30	−10.18	−9.11

[a]Distance in Base Pairs from the beginning of the 3'UTR of each gene

[b]PITA's "X:Y:Z" notation for describing the seed represents the size of the seed (X), the number of mismatches (Y) and the number of G:U wobble pairs (Z).